European Polymer Journal 64 (2015) 1–9

Contents lists available at ScienceDirect

European Polymer Journal

journal homepage: www.elsevier.com/locate/europolj

Viscoelastic response of linear defects trapped in polymer networks

Leandro E. Roth [a], Diana C. Agudelo [a], Jorge A. Ressia [a], Leopoldo R. Gómez [b], Enrique M. Vallés [a], Marcelo A. Villar [a], Daniel A. Vega [b,*]

[a] Department of Chemical Engineering, Planta Piloto de Ingeniería Química, Camino La Carrindanga Km. 7, Universidad Nacional del Sur, CONICET, 8000 Bahía Blanca, Argentina
[b] Department of Physics, Instituto de Física del Sur (IFISUR), Universidad Nacional del Sur, CONICET, Av. L.N. Alem 1253, 8000 Bahía Blanca, Argentina

ARTICLE INFO

Article history:
Received 3 October 2014
Received in revised form 23 December 2014
Accepted 24 December 2014
Available online 31 December 2014

Keywords:
Model networks
Viscoelastic properties
Network defects
Rubber elasticity

ABSTRACT

We analyze the dynamic response of end-linked poly(dimethylsiloxane) networks containing entangled unattached guest linear polymers. Upon increasing the content of unattached guest polymers there is an increasing dissipation and a reduction in the network elasticity. It was found that the width of the relaxation spectrum is nearly insensitive to the content of guest chains, indicating that the network structure is not affected by the presence of these defects and that the effective number of entanglements associated to guest chains is independent of the equilibrium elastic modulus of the networks.

The inhibition of the constraints release mechanism for molecules trapped in polymer networks have enormous consequences on the dynamic response, producing a dramatic slowing down in the relaxational dynamics of defects. The presence of different structures of defects in polymer networks is physically unavoidable, even under optimum reaction conditions. Here we found that the slow dynamics of soluble branched structures or dangling molecules can easily hide the contribution of linear unattached molecules.

1. Introduction

Viscoelastic and diffusional properties of entangled polymers have been successfully described by the tube model [1–8]. According to this model, the topological confinement exerted on a given molecule by the surrounding media can be modeled as a hypothetical tube that severely suppress the motion perpendicular to the tube's local axis, but permits the diffusion along the tube [3,4].

For linear chains, the long time dynamics is mainly controlled by the diffusion of molecules along its own contour, a process known as "reptation" [1]. In this case, the theory predicts that both, terminal relaxation time τ_d and shear zero viscosity η_0 scales with the molar mass of the linear polymer chain M as $\tau_d \sim M^3$ and $\eta_0 \sim M^3$, respectively. However, several experimental studies clearly indicate a stronger dependence on molar mass, with both quantities scaling as $M^{3.4}$ [4–6]. Then, in addition to the dominating effect of chain reptation, two additional mechanisms must be considered in order to obtain a quantitative agreement with the experiments [4–6,9]: *contour-length fluctuations* and *constraint release*. Contour length fluctuations [8] account for the shortening of the primitive path as a result of fast random motions of the chain ends while the constraint release mechanism takes into account the fact that some of the chains that define the confining tube release their constraints [4–6].

Unlike a linear chain, branched molecules cannot reptate to recover equilibrium. In this case, reptation is severely suppressed and chains renew their configurations mainly through arm retraction [2,4–6,10–19]. In this case

* Corresponding author.
E-mail address: dvega@criba.edu.ar (D.A. Vega).

http://dx.doi.org/10.1016/j.eurpolymj.2014.12.036
0014-3057/

the end of each arm must retract partway down its confining tube to reemerge along a different path [4]. The absence of reptation due to the branching point has important consequences on the dynamics of branched polymers in both, the linear [4–6] and non-linear viscoelastic regimes [20–27]. Quite differently from the power law observed for linear polymers, arm retraction mechanism is highly unfavorable and the time scale for complete retraction in the entangled regime increases roughly exponentially with the molar mass of the branch [2,4]. This mechanism was firstly studied by de Gennes, who considered the motion of a symmetric star shaped polymer in a fixed network of obstacles and showed that the probability for a star arm of length N to retract fully to the junction point is exponentially unlikely. Then, the longest relaxation time that allows the star arm to completely lose its configurational memory becomes $\tau_s \sim \exp(\gamma N)$, where γ is a constant [2].

Stress relaxation of symmetric star polymers in a fixed network of obstacles was theoretically studied through the tube model formalism by Doi and Kuzuu [11] and Pearson and Helfand [12]. According to this model the arm free end can be thought to be undergoing Brownian motion in a potential field dictated by the effective number of entanglements per star arm. The Pearson–Helfand model predicts that the arm potential $U_{PH}(s)$ has the following quadratic form [4,12]: $U_{PH}(s) = \frac{15}{8} Z s^2$, where $s(0 < s < 1)$ is the fractional distance back along the primitive path where the arm free end has been retracted and Z is the average number of entanglements per star arm [5,16]. Within this theoretical frame, the terminal relaxation time for a star trapped in a fixed network of obstacles results [28,29]:

$$\tau_{PH}(s, n_e) = -\frac{1}{2} I \pi^3 Z^2 \tau_e \, erf(I\sqrt{v Z} s) \quad (1)$$

where $v = 15/8$ $I = \sqrt{(-1)}$, $erf[x]$ is the error function and τ_e is the Rouse relaxation time for an entanglement segment [4,5].

When compared with experiments employing symmetric star polymer melts with different chemical structure, it has been shown that the Pearson–Helfand potential largely over-predicts the terminal relaxation time [4,15,16]. Then, in order to remove the discrepancy between the theory ($\tau_{PH}(n_e) \sim \exp[15/8Z]$) and experiments ($\tau_{exp}(Z) \sim \exp[0.6Z]$), it is necessary to reduce the strength of the arm retraction potential by a factor of about 3 [4,16,18]. This discrepancy was solved by considering not only arm retraction process but also the constraint release contribution. In a melt of entangled star shaped molecules, different arms are not moving in a fixed network of obstacles since some topological constraints can be released by other star free ends in the neighborhood. In this case the constraint release mechanism contributes to speed up the relaxational dynamics [4,6].

On the other hand, during the last decades the dynamics of macromolecules trapped in polymer networks have attracted considerable attention due to their practical and theoretical interest [28,30–41]. Since in polymer networks the confining tube remains nearly invariant, the process of constraint release is inhibited [28]. Consequently, polymer networks can be employed as an excellent model to study the dynamics of polymers with different architectures in the absence of this important relaxational mechanism. For example, a guest linear chain trapped in a network will lose its conformational memory mainly via reptation [42–47] while the slow relaxation of a symmetric star or a linear pendant chain [28,48–57] is driven by arm retraction in the very strong arm retraction potential $U_{PH}(s)$ [28].

In this work, we employ well characterized PDMS networks with controlled amounts of unattached linear guest polymers to analyze their influence on the viscoelastic response. The results are theoretically rationalized in terms of the tube model and compared with available data for networks containing similar amounts of linear dangling chains.

Although the problem of linear guest chains trapped in a network has been previously explored to test the validity of the tube model [42–47], here we focus the attention on the effect of guest chains concentration on the elastic and dissipative properties. The role of unavoidable defects residing in the network structure and their contribution to the dynamic response is also analyzed.

2. Experimental

Model poly(dimethylsiloxane) networks were obtained by a hydrosilylation reaction, based on the addition of hydrogen silanes from cross-linker molecules to end vinyl groups present in prepolymer molecules [49,58–61]. A commercial difunctional prepolymer, α,ω-divinyl poly(dimethylsiloxane) (B_2) (United Chemical Technology, Inc.) and linear unreactive poly(dimethylsiloxane) polymers ($B_{0,1-4}$) with different molar masses were employed. The molar mass characterization of the prepolymers and other reactants used in the cross-linking reactions are listed in Table 1 where the notation $B_{0,i}$, with $i = 1–4$, was employed for the linear poly(dimethylsiloxane) chains. Phenyltris(dimethylsiloxy)silane (A_3) (United Chemical Technology, Inc.) was used as cross-linker and a Pt salt was employed as catalyst for the cross-linking reaction.

Four linear polymers ($B_{0,i=1-4}$) with relatively narrow molar mass distribution were obtained from monofunctional polymers synthesized previously by anionic polymerization, using n-butyllithium as initiator, n-hexane as solvent and tetrahydrofuran (THF) as polymerization promoter. The vinyl group chain end of the monofunctional polymers was neutralized by a hydrosilylation reaction with a monofunctional reagent containing a silane group (A_1). The monofunctional reagent A_1 employed was pentamethyldisiloxane, which was used in excess of about 100%. A Pt salt was used as catalyst for the reaction. The neutralization reaction was carried out in solution, using toluene as solvent for about 24 h. The reactive mixture was maintained under nitrogen atmosphere with mechanical stirring at a temperature of 333 K. Once the reaction was completed, the polymer was precipitated from the reaction media using methanol. The PDMSs without reactive groups was then separated from the solvent and dried under vacuum up to constant weight. The elimination of

Table 1
Molecular characterization of linear prepolymers and other reactants used for the preparation of model PDMS networks.

PDMS (linear)	Mn (SEC) (g/mol)	Mw (SEC) (g/mol)	Mw/Mn	η_0 (Pa s)	τ_d[b] (10^{-3} s)
B_2	7300	21,300	2.95	0.3	0.001
$B_{0,1}$	47,800	51,300	1.07	4.3	0.02
$B_{0,2}$	97,200	121,000	1.24	110	0.5
$B_{0,3}$	136,000	168,000	1.24	290	1.4
$B_{0,4}$	224,000	269,000	1.20	1280	6.4
$B_{1,1}$[a]	47,800	51,300	1.07	4.3	0.02
$B_{1,2}$[a]	97,200	121,000	1.24	220	0.5

[a] Data from Ref. 60.
[b] Estimated as $\tau_d = \eta_0/G_0$, where $G_0 = 2 \times 10^5$ Pa is the plateau modulus for entangled PDMS melts [62].

the reactive end in monofunctional polymers was verified by Fourier transform infrared spectroscopy (FTIR), through the absence of one characteristic peak absorption of vinyl groups (stretching at 4.650 cm^{-1}).

The prepolymer B_2 and the cross-linker were weighted in order to obtain stoichiometrically balanced mixtures. To prepare the networks (see the scheme of Fig. 1), the blend of precursors B_2, the cross-linker A_3 and the unreactive polymers $B_{0,i}$ were mechanically stirred for 2 h. The composition of the different systems employed in the synthesis of model networks containing linear guest chains is shown in Table 2.

Reactants were mixed with a mechanical stirrer and degassed under vacuum to eliminate bubbles. The reactive mixture was then placed between the plates of a mechanical spectrometer (Rheometrics Dynamic Analyzer RDA-II). Cure reactions were carried out at 333 K and final properties were measured after 24 h of reaction. Dynamic measurements were done, under nitrogen atmosphere, in the temperature range of 243–473 K using 25-mm parallel plates. Elastic modulus, $G'(\omega)$, and loss modulus, $G''(\omega)$, in the range of 0.05–500 rad/s were obtained with deformations of up to 20% within the range of linear viscoelastic response. Similar experimental conditions were employed to characterize the rheological behavior of the melts of linear guest polymers $B_{0,1-4}$.

It is worthwhile noting, that polymer networks prepared for this study have as small contents of undesired structural defects as possible. As pointed out in previous studies, the molecular structure of a polymeric network is strongly influenced by the final extent of reaction reached during the cross-linking process. It has been found that even stoichiometrically balanced networks at near complete reaction contain defects. Consequently, in any real system there are a small content of solubles and pendant chains that affect the viscoelastic response [39,55].

Since the concentration of $B_{0,i}$ chains considered in this study is relatively small (see Table 2), it can be expected that only a small fraction of these chains become involved in self-entanglements. In order to estimate the fraction of self entanglements among linear guest chains we can consider the dependence of the effective entanglement molar mass on polymer concentration ϕ. It has been found in entangled polymer melts diluted by theta-solvents that molar mass between entanglements $M_e(\phi)$ depends on polymer concentration ϕ as $M_e(\phi) = \frac{M_e^{melt}}{\phi^{4/3}}$ [5,16]. Here

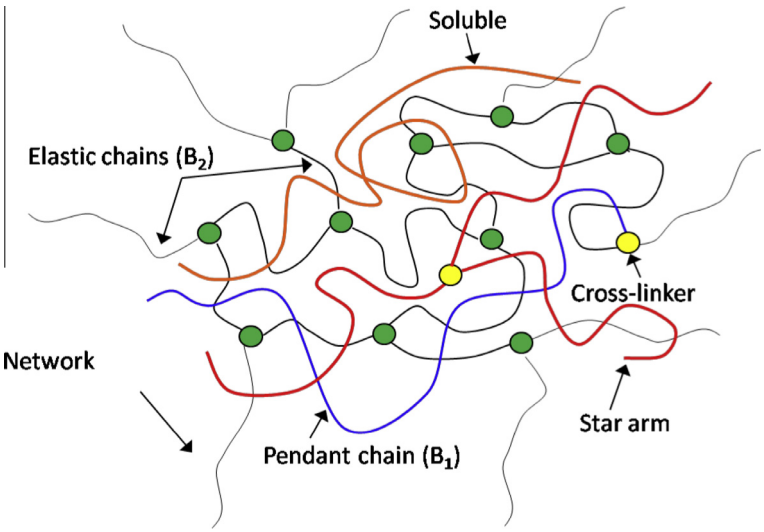

Fig. 1. Schematic representation of model silicone networks obtained via the end-linking technique. Here soluble linear molecules B_0 are indicated with an orange line, the cross-linkers with circles (green) and the difunctional chains B_2 with black lines. Linear pendant chains (B_1) are linked to the network structure only through one of the chain ends (blue line). The rheological behavior of pendant chains is similar to trapped stars (red lines) with the same arm molar mass. (For interpretation of the references to color in this figure legend, the reader is referred to the web version of this article.)

Table 2
Nomenclature and main features of the networks.

Network	Defect	Mw_{B0} (g/mol)	w_{B0} (g/g)	$G'_{\omega\to 0}$* (MPa)	Z†	$Z\,w_{B0}^{4/3}$	M_{eff} (g/mol)
B_2–00	None	–	–	0.265	3	–	8300
B_2–$B_{0,1}$–01	Guest	51,300	0.010	0.251	5	<0.1	8800
B_2–$B_{0,1}$–03	guest	51,300	0.029	0.241	5	<0.1	9100
B_2–$B_{0,1}$–05	Guest	51,300	0.049	0.230	5	<0.1	9600
B_2–$B_{0,1}$–10	Guest	51,300	0.098	0.214	5	0.2	10,300
B_2–$B_{0,1}$–15	Guest	51,300	0.146	0.183	5	0.4	12,000
B_2–$B_{0,1}$–20	Guest	51,300	0.196	0.173	5	0.6	12,700
B_2–$B_{0,2}$–01	Guest	121,000	0.011	0.244	12	<0.1	9000
B_2–$B_{0,2}$–03	Guest	121,000	0.031	0.238	12	0.1	9250
B_2–$B_{0,2}$–05	Guest	121,000	0.049	0.228	12	0.2	9700
B_2–$B_{0,2}$–10	Guest	121,000	0.099	0.205	12	0.6	10,800
B_2–$B_{0,2}$–15	Guest	121,000	0.148	0.189	12	1.0	11,600
B_2–$B_{0,2}$–20	Guest	121,000	0.196	0.159	12	1.4	13,800
B_2–$B_{0,3}$–10	Guest	168,000	0.10	0.187	17	0.8	11,800
B_2–$B_{0,4}$–10	Guest	269,000	0.10	0.197	27	1.3	11,200
B_2–$B_{1,1}$–10‡	Pendant	51,300	0.996	0.197	5	<0.1	11,200
B_2–$B_{1,2}$–10‡	Pendant	121,000	0.101	0.197	12	0.2	11,200

* Here $G'_{\omega\to 0}$ is the storage modulus in the limit of low frequencies.
† Estimated through Mw considering $M_e = 10^4$ g/mol.
‡ Data from Ref. 62.

M_e^{melt} is the molar mass between entanglements in the melt. Thus, under dilution the effective number of entanglement of a linear polymer of molar mass M results: $Z(\phi) = \frac{M}{M_e(\phi)} = \frac{M}{M_e^{melt}}\phi^{4/3}$. Table 2 shows the effective number of entanglements expected for linear guest chains in a melt (in this study elastic chains B_2 have a molar mass similar to M_e in a melt of the guest chains) and the number of self-entanglements calculated as $Z(w_{B0}) = \frac{M}{M_e}w_{B0}^{4/3}$, where w_{B0} is the weight fraction of guest chains. The molar mass between entanglements can estimated through the plateau modulus G_0 as: $G_0 = \frac{4}{5}\rho RT/M_e^{melt}$, where ρ is the polymer density, R is the universal gas constant, T is the absolute temperature (see Refs. [5,63] for more a detailed discussion about the relationship between G_0 and M_e^{melt}). Here we considered $M_e^{melt} \approx 10^4$ g/mol [62].

Note that even at the highest polymer concentration (20 wt%) the probability of self-entanglements among guest chains remains small. Therefore, one can expect that the possibility of constraint release due to self-entanglements between guest chains remains small in the whole set of polymer networks studied.

3. Results

Figs. 2 and 3 show the master curves of storage (G') and loss modulus (G'') as a function of frequency (ω) for networks prepared with different contents of linear guest chains $B_{0,1}$ and $B_{0,2}$.

As shown in Fig. 2 and Table 2, the equilibrium modulus ($G'_{\omega\to 0}$) decreases as the content of guest chains increases. This behavior is emphasized in Fig. 4, that compares G' at a fixed frequency of 1 rad/s as function of the content of guest chains for different networks.

Upon adding 20 wt% of guest chains, the elastic modulus drops by a factor of about 0.65 and 0.6 for networks prepared with unattached polymer chains $B_{0,1}$ and $B_{0,2}$ respectively. This reduction in the elastic modulus can be attributed to the "solvent-like" effect of the guest chains that, in the low frequency regime, cannot contribute to the elastic response. The dependence of $G'_{\omega\to 0}$ with polymer concentration is consistent with the theory for semidilute theta solutions, which predicts that the plateau modulus G_0 of well entangled polymer melts scales as $G_0 \sim \phi^{(7/3)}$ [5,16,64]. For example, for networks with 20 wt% of unattached linear chains we have $(1-0.2)^{7/3} \approx 0.59$, which is consistent with the reduction in $G'_{\omega\to 0}$ observed in Figs. 2 and 4. This is a very interesting result that indicates that at maximum extent of reaction, network architecture is not severely affected by the presence of unattached material. Therefore, contrary to pendant material that reduces the content of elastically active cross-links and the network elasticity [59], here guest chains appears to behave as a solvent in the low frequency regime.

At low frequencies guest chains are relaxed and cannot contribute to the elasticity of the network. As the frequency increases, an increasing fraction of these molecules contributes to the elastic response. That is, as the time scales of exploration become smaller than their terminal relaxation times, larger contents of defects and unattached guest chains become elastically active.

In the high frequency regime the relaxational dynamics involves segmental motions of the different constituents of the network. Then, transiently trapped entanglements associated to structural defects and guest chains may contribute to the networks elasticity at time scales above their terminal relaxation times. In Fig. 2 it can be observed that elastic modulus is a monotonously growing function of the frequency. While for networks with the shorter guest chains the increment in $G'(\omega)$ in the frequency range 10^{-2}–10^4 rad/s is nearly insensitive to the content of linear guest polymers, the response of the networks with the larger chains $B_{0,2}$ are markedly different due to their slower dynamics.

In a perfectly elastic network the loss modulus should be negligible except in the high frequency regime, where Rouse-like relaxation modes lead the dynamics. Rheological

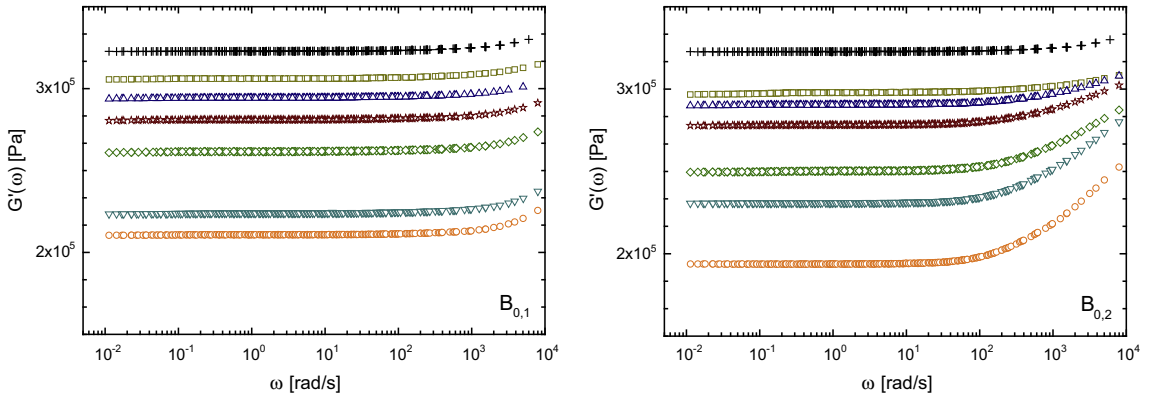

Fig. 2. Master curves of storage modulus (G') as a function of frequency (ω). Networks prepared with different contents of guest chains $B_{0,1}$ (left) and $B_{0,2}$ (rigth). Symbols: (+) 0 wt%, (□) ~1 wt%, (△) ~3 wt%, (☆) ~5 wt%, (◇) 10 wt%, (▽) 15 wt%, and (○) 20 wt%. $T_0 = 273$ K.

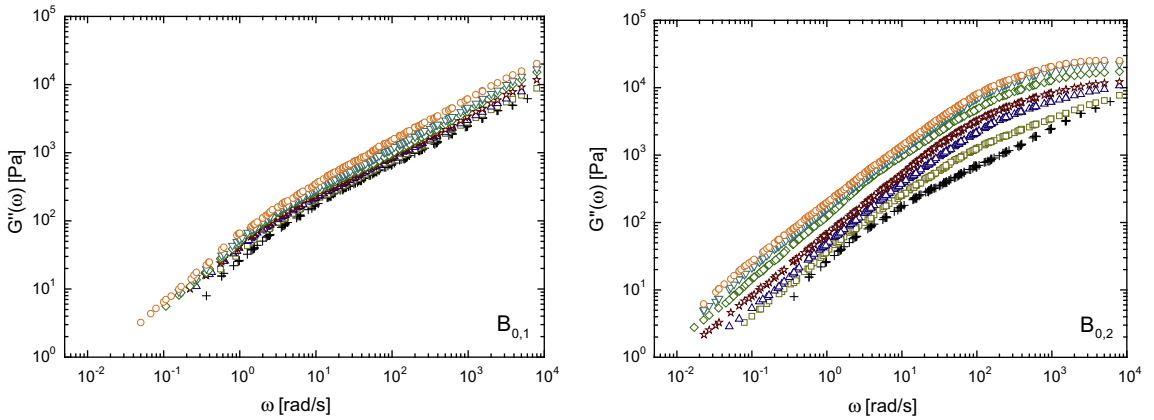

Fig. 3. Master curves of loss modulus (G'') as a function of frequency (ω). $T_0 = 273$ K. Networks prepared with different contents of guest chains $B_{0,1}$ (left) and $B_{0,2}$ (right). Symbols: same as Fig. 2.

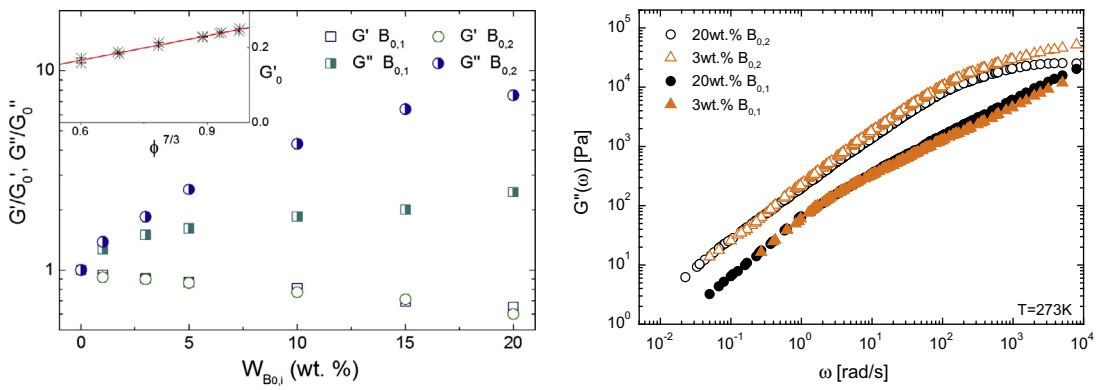

Fig. 4. Left panel: Storage (open symbols) and loss modulus (filled symbols) at a frequency of $\omega = 1$ rad/s normalized with the value corresponding to the "defect free" network $A_3 + B_2$ (G_0' and G_0''). Note that if the content of guest chains increases, there is a small reduction in the elasticity but a strong increment in the loss modulus. The inset shows G_0' as a function of $\phi = (1 - w_{B0})$. Observe that G_0' is roughly linear with $\phi^{7/3}$ (continuous line). Right panel: Loss modulus as a function of frequency (ω) at $T_0 = 273$ K for networks prepared with unattached chain $B_{0,1}$ (filled symbols) and $B_{0,2}$ (open symbols). Triangles represent the data of networks containing 3 wt% of unattached linear chains rescaled to compare with the data corresponding to networks with 20 wt% of guest chains. In order to overlap the curves, data corresponding to networks prepared with 3 wt% of unattached material was multiplied by factors of 1.5 and 4.5 for networks containing $B_{0,1}$ and $B_{0,2}$ chains, respectively.

and Double Quantum Proton Nuclear Magnetic Resonance experiments show that the main contributions to the loss modulus observed in stoichiometrically balanced end-linked networks come from the pendant material that is produced in the network [39,61]. Non idealities, such as the presence of small contents of non-reactive polymer precursors, steric effects and local inhomogeneities limit the maximum extent of reaction. Numerous experiments indicate that even at the optimum reaction conditions the content of soluble material in the network cannot be reduced below ~2–3 wt% [39,61]. Therefore, as the maximum extent of reaction p_∞ at long reaction times hardly overcomes $p_\infty = 0.94$, polymer networks always present a small content of pendant and soluble material. Although these defects may have a complex branched architecture, in the system $A_3 + B_2$ (without added defects B_0 or B_1) NMR studies and mean field calculations [39] indicate that most of the solubles are constituted by unreacted linear B_2 chains while the larger contribution to the dangling material comes from the linear pendant chains formed as a consequence of the partial reaction of the precursors B_2 that are attached to the network only through one chain end (see scheme of Fig. 1).

In order to provide an estimation of the relaxation times associated to polymers with different architectures, Fig. 5 compares the theoretical terminal relaxation time for linear polymers ($\tau_0 \sim \tau_e Z^3 (1 - 1/\sqrt{Z})^2$) [4,9] and stars trapped in a fixed network of obstacles (Eq. (1)). It is worth mentioning that star polymers trapped in a network have essentially the same relaxation spectrum of linear pendant chains with the same molar mass of the star arm [28]. For comparison, the relaxation time corresponding to star melts is also included (see Refs. [16,18] for more details). Note that even for moderately entangled polymers the difference in terminal relaxation times can be surprisingly large.

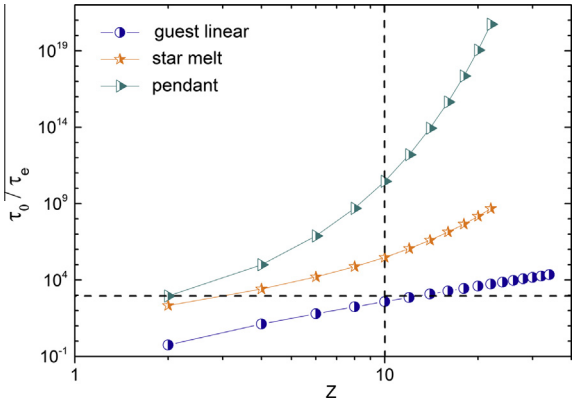

Fig. 5. Terminal relaxation time as a function of the effective number of entangled segments for symmetric star shaped and linear polymer chains trapped in a polymer network. Theoretical results for star melts are also included for comparison. In the case of stars, Z corresponds to the number of entanglements per star arm. The horizontal dashed line serves as a guide to the eye to compare the number of entanglements associated to different defects in order to produce an equivalent terminal relaxation time.

For example, while for a free linear chain involving 10 entanglements the terminal relaxation time is about 10^3 τ_e, for a pendant chain trapped in a network this relaxation time becomes larger by nearly 8 orders of magnitude!

Due to the large difference in relaxation times (see Fig. 5), it is possible to note that although both defects, pendants (partially reacted B_2 chains) and linear soluble (unreacted B_2 chains), contribute to the dynamic modulus, in the frequency regime explored here, for the system $A_3 + B_2$ only pendant chains may show up at these time-scales. Consequently, in $A_3 + B_2$ networks the main contribution to the observed loss modulus comes from linear pendant chains produced by partially attached to the network B_2 molecules (see Fig. 3). The slight increment of the storage modulus observed for this system in the high frequency regime can also be attributed to the contribution of pendant chains B_2.

When compared to the system $A_3 + B_2$, loss modulus increases with the content of unattached chains and with the average molar mass of these defects (Fig. 3). In network containing shorter $B_{0,1}$ chains the relaxational spectrum is essentially undistinguishable from the one corresponding to networks prepared without guest chains ($A_3 + B_2$), except for a slight vertical shift. In this case the terminal relaxation time of the guest chains is small as compared to the one corresponding to dangling chains B_2 produced during the reaction. Then, at the time scales explored here the contribution of these guest chains is severely hidden by the pendant material produced by partially reacted B_2 chains. On the other hand, upon the addition of unattached chains $B_{0,2}$ networks increase notoriously its dissipative behavior. However, similarly to networks with guest chains $B_{0,1}$ their relaxation spectrum appears to be insensitive to their content, except for an increment in the loss modulus as the content of unattached material increases.

The terminal relaxation time of guest chains in the melt can be estimated as $\tau_d \sim \eta_0 / G_0$, where $\eta_0 = \lim_{\omega \to 0} \frac{G''(\omega)}{\omega}$ is the zero shear rate viscosity and G_0 the plateau modulus [4]. Table 1 shows the terminal relaxation time in the melt for different guest chains employed in this study, considering $G_0 = 0.2$ MPa as the plateau modulus for PDMS [62]. Note that the terminal relaxation time in the melt is $\tau_d \sim 2 \times 10^{-5}$ s and $\tau_d \sim 5 \times 10^{-4}$ s for chains $B_{0,1}$ and $B_{0,2}$, respectively. Then, in the terminal region of G'' it can expected that, as compared with the networks with $B_{0,1}$ the data corresponding to networks containing $B_{0,2}$ become shifted toward the low frequency regime by a factor of about 25. However, in Fig. 3 can be observed that, at a fixed concentration of guest chains, this shift factor is only about 3 since the contribution of $B_{0,1}$ chains is hidden by the pendant material coming from the partially attached B_2 chains.

The right panel of Fig. 4 compares the loss modulus for networks containing 3 wt% and 20 wt% of linear guest chains. Note that upon a vertical rescaling of $G''(\omega)$ for the networks containing 20 wt% of guest chains, the relaxation spectrum overlaps quite nicely over a wide range of frequencies with the data corresponding to the networks containing 3 wt% of guest chains. Thus, as previously discussed, the effect of self-entanglements between guest chains must be quite small since their distribution of

relaxation times is roughly independent of the molar mass content of the unattached material (although obviously it depends on the molecular mass distribution of the guest chains). Fig. 4 also compares $G''(\omega)$ at a frequency of 1 rad/s as a function of the content of guest chains $B_{0,1}$ and $B_{0,2}$, normalized with the respective modulus measured in networks without guest chains. Note that upon the addition of 20 wt% of linear guest chains $B_{0,2}$ loss modulus increases by almost one order of magnitude above the value corresponding to the network without guest chains, indicating that through the addition of small contents of well entangled guest chains it should be possible to finely tune the loss modulus without seriously affecting the elastic response.

4. Discussion

A direct comparison among experiments and theoretical predictions of tube models for the viscoelasticity of polymer chains trapped in a permanent network requires of an adequate estimation of the average molar mass between entanglements in the network M_e^{net}. Although a comparison between the predictions of the classical theory of rubber elasticity and tube models for polymer melts may suggest that M_e^{melt} could be correlated to $G'(\omega)_{\omega\to 0}$ and G_0, a direct estimation is not simple.

As pointed out above, in a polymer melt M_e^{melt} is usually defined in terms of the plateau modulus G_0 as: $M_e^{melt} = \frac{4}{5}\frac{\rho RT}{G_0}$ [4–6,63]. In this case, for a linear chain of average molar mass M, the average number of entanglements results $Z^{melt} = M/M_e^{melt}$. Similarly, if the molar mass M_x of the elastic chains B_2 connecting the cross-linking points of the network is large as compared with the molar mass between entanglements in a melt M_e^{melt}, it can be expected that the number of entanglements associated to a guest chain to be the same as in its own melt, i.e., $Z^{melt} = Z^{net}$. On the other hand, if $Mx < Me^{melt}$ or $Mx \sim Me^{melt}$ the effective number of entanglements in the network Z^{net} can increase above Z^{melt} ($Z^{melt} < Z^{net}$). However, in this case the connection between Mx and M_e^{melt} is not simple since network structure can led to more or less tight confining tubes depending on a number of parameters, including the functionality of the cross-linkers, density of defects, maximum extent of reaction, etc.

The equilibrium modulus G_0 of polymer network depends primarily on the density of elastically effective chains and cross-links with an additional contribution coming from trapped entanglements. Theoretical predictions of this modulus can be obtained based on the theory of elasticity: [49,51]

$$G_0 = RT[\nu - h\mu] + G_e T_e \qquad (2)$$

where ν is the concentration of elastically active chains, h an empirical constant (taking values between 0 and 1, depending upon the degree of fluctuations of the cross-linker points), μ the concentration of cross-linking points, R the gas constant, and T the absolute temperature. In this model T_e is the fraction of trapped entanglements and G_e is the contribution to the modulus by the trapped entanglements.

As there is no experimental method to determine accurately the network architecture, the five parameters in Eq. (2) are obtained indirectly through rheological and swelling experiments combined with mean field models. The complexity of the above equation can be partially reduced by considering the following three parameters equation:

$$G_0 \approx \rho RT\left[\frac{1}{M_x} + \frac{\alpha}{M_e^{net}}\right] = \frac{\rho RT}{M_{eff}} \qquad (3)$$

where Mx is the average molar mass of the elastically active polymer chains connecting cross-linkers (in our case mainly determined by B_2 chains), M_e^{net} is the average molar mass between entanglements in the network (which does not necessarily coincides with M_e^{melt}), α is a factor that accounts for the contribution of entanglements and M_{eff} is an effective molar mass that include both, elastic strands and entanglement contributions.

Although a correct estimation of the fraction of trapped entanglements contribution to network elasticity is far from being trivial, M_{eff} can be directly determined through the measured equilibrium modules (see Table 2). Note that in the networks studied here, M_{eff} changes from $M_{eff} \approx 8,000$ g/mol for networks without added defects to $M_{eff} \approx 14,000$ g/mol for networks with 20 wt% of guest chains. However, previously we pointed out that the relaxation spectrum is insensitive to the content of guest chains (see Fig. 4), indicating that for different networks there are no important changes in the average number of entanglements in which defects are involved and then, that the tube dimensions are not being altered by the guest chains.

Then, although the B_2 precursor employed to generate elastic chains has an average molar mass that is slightly smaller than M_e^{melt} (see Tables 1 and 2) the diameter of the confining tube appears to be the same as in the melt ($Z^{net} = Z^{melt}$).

In order to obtain a rough estimation about the effects of network structure on the dynamic of guest chains,

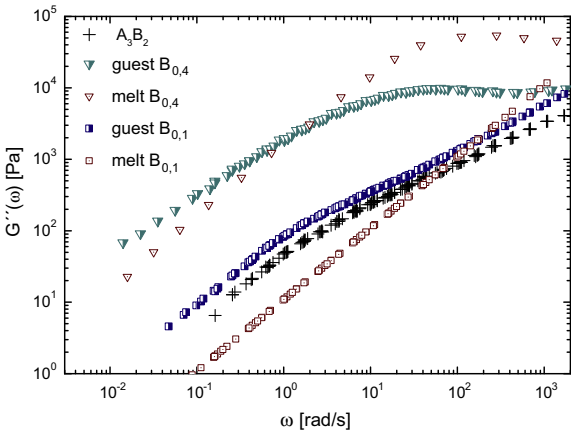

Fig. 6. Master curves of loss modulus (G'') as a function of frequency (ω) for melts of linear PDMS chains (open symbols) and for networks prepared with 10 wt% of PDMS guest chains. Data corresponding to the "defect free" network (+) are included for comparison. T_0 = 273 K.

Fig. 6 shows the loss modulus for polymer networks prepared with 10 wt% of chains $B_{0,1}$ and $B_{0,4}$. In the figure it has been also included the loss modulus of molten linear polymer chains.

It can be observed that in both cases, guest chains in the networks show a slower dynamics as compared with their corresponding melts (as compared with their melts, guest chains in the networks present a shift toward the low frequency regime). Given that chains $B_{0,1}$ have a relatively small molar mass, G'' does not show a maximum in the frequency regime explored in this work. Therefore, for this system is not possible to clearly identify the effective frequency shift produced by the trapping effect of the network. On the other hand, for the systems involving chains $B_{0,4}$, in both the network and the melt, G'' exhibits a maximum. As compared with their melt, the maximum in G'' shifts toward the low frequency regime by a factor of about 5, in agreement with previous data of the literature for polybutadiene chains trapped in rubber networks [65].

Fig. 7 compares the loss modulus for polymer networks prepared with 10 wt% of guest chains with different molar mass ($B_{0,i}$, i = 1–4). This figure also includes literature data corresponding to networks prepared with 10 wt% of pendant chains $B_{1,1}$ and $B_{1,2}$ (see Ref. [60] and Table 1 for details about their molar masses).

Since pendant chains behave as star polymers trapped in a network [28], their dynamics is dictated by arm retraction. Thus, as shown in Fig. 5, even for moderately entangled systems the terminal relaxation time of pendant or star chains can be larger by several orders of magnitude than the corresponding to linear chains. This feature is clearly observed in Fig. 7, where the network with linear pendant chains $B_{1,1}$ shows a quite broader relaxational spectrum than the corresponding to linear guest chains $B_{0,1}$, even so both defects have the same molar mass. Indeed, note that in the low frequency region, pendant chains $B_{1,1}$ that involve an average of about 5 entanglements (see Table 2) present a similar behavior that networks prepared with guest linear chains $B_{0,4}$, that present 27 entanglements!

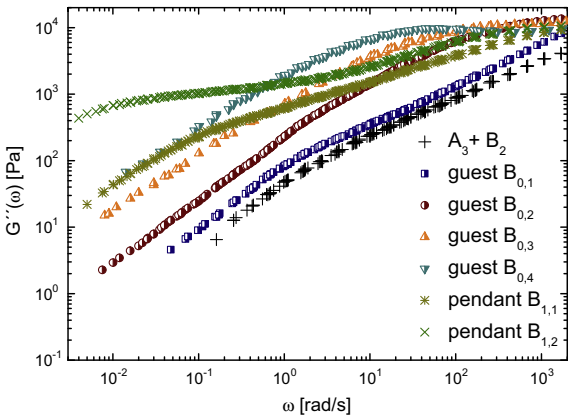

Fig. 7. Master curves of loss modulus (G'') as a function of frequency (ω) for networks prepared with 10 wt% of guest or pendants chains. Symbols: (+) $A_3 + B_2$, (■) guest $B_{0,1}$ chains, (●) guest $B_{0,2}$ chains, (▲) guest $B_{0,3}$ chains, (▼) guest $B_{0,4}$ chains, (✳) pendant $B_{1,1}$ chains, and (×) pendant $B_{1,2}$ chains. T_0 = 273 K.

Fig. 7 also shows that the addition of low contents of moderately entangled pendant material have an enormous consequence of their dissipative dynamics and are largely more effective to enhance the damping properties than guest chains. Although in both cases the addition of a 10 wt% of defects reduce the storage modulus by about 20%, in the networks with pendant chains the loss modulus remains more insensitive to the frequency than the corresponding to guest linear chains with the same molar mass. On the other hand, while networks with pendant chains $B_{1,2}$ show a loss modulus decay of about one order of magnitude in the frequency range between 10^{-3} and 10^{3} rad/s, in networks with guest chains $B_{0,2}$ there is a loss modulus decay of nearly four orders of magnitude.

5. Conclusions

Model polymer networks can be employed as an excellent model to test the dynamics of polymer chains with different architectures in the absence of the constraint release mechanism. However, in order to compare experimental data with theory, two important aspects should be taken into account: the slow relaxation of the unavoidable pendant material and the effective tube diameter. While in a melt the tube diameter is primarily determined by the chemical architecture of the polymer, in a network the confining tube can be also affected by network architecture. Here we have observed that although the precursor employed to generate elastic chains has a number average molar mass M_n that is slightly smaller than M_e^{melt} the diameter of the confining tube appears to be the same as in the melt. According to the tube model theories, pendant material involves a relaxational process drastically slower than the corresponding to linear unattached chains with similar molar mass. Then, pendant chains can easily hide the contribution of linear guest chains over a wide range of molar masses. PDMS end-linked networks employing difunctional chains with molar mass of approximately 5×10^4 g/mol will unavoidably contain pendant chains involving about 5 entanglements ($Z \sim 5$). These pendant chains will severely hide the contribution of any guest chain with molar mass below 2×10^5 g/mol ($Z \sim 20$). For example, we have observed here that in the low frequency regime linear pendant chains involving an average of ~5 entanglements present a similar behavior that networks prepared with linear guest chains with ~30 entanglements. Then, any comparison with reptation models should be aware of the role of pendant material in the dynamic. Although this undesirable contribution can be reduced by an adequate selection of the molecular weights of the network precursors and guest chains, special attention should be paid to their quite different relaxational mechanisms of energy dissipation.

As the dissipative behavior of a network can be increased by several orders of magnitude by adding controlled amounts of defects without severely affecting its elasticity, an accurate control over the network architecture may allow to obtain viscoelastic materials with prescribed properties over a wide range of time-scales.

Acknowledgements

We express our gratitude to the Universidad Nacional del Sur (UNS) and the National Research Council of Argentina (CONICET) which supported this work.

References

[1] de Gennes PG. J Chem Phys 1971;55:572–9.
[2] de Gennes. Scaling concepts in polymer physics. Ithaca, New York: Cornell University Press; 1979.
[3] Doi M, Edwards SF. J Chem Soc, Faraday Trans 1978;74:1789–801.
[4] Doi M, Edwards SF. The theory of polymer dynamics. Oxford: Clarendon Press; 1986.
[5] McLeish TCB. Adv Phys 2002;51:1379–527.
[6] Watanabe H. Prog Polym Sci 1999;24:1253–403.
[7] Qin J, Milner ST. Macromolecules 2013;46:1659–72.
[8] Doi M. J Polym Sci 1983;21:667–84.
[9] Milner ST, McLeish TCB. Phys Rev Lett 1998;81:725–8.
[10] Graessley WW, Masuda T, Roovers JEL, Hadjichristidis N. Macromolecules 1976;9:127–41.
[11] Doi M, Kuzuu NY. J Polym Sci Lett 1980;18:775–80.
[12] Pearson DS, Helfand E. Macromolecules 1984;17:888–95.
[13] Needs RJ, Edwards SF. Macromolecules 1983;16:1492–5.
[14] Bartels CR, Crist B, Fetters LJ, Graessley WW. Macromolecules 1986;19:785–93.
[15] Ball RC, McLeish TCB. Macromolecules 1989;22:1911–3.
[16] Milner ST, McLeish TCB. Macromolecules 1997;30:2159–66.
[17] Frischknecht AL, Milner ST, Pryke A, Young RN, Hawkins R, McLeish TCB. Macromolecules 2002;35:4801–20.
[18] Vega DA, Sebastian JM, Russel WB, Register RA. Macromolecules 2002;35:169–77.
[19] Miros A, Vlassopoulos D, Likhtman AE, Roovers J. J Rheol 2003;47:163–76.
[20] Laun HM. Rheol Acta 1978;17:415–25.
[21] Osaki K, Kurata M. Macromolecules 1980;13:671–6.
[22] Samurkas T, Larson RG, Dealy JM. J Rheol 1989;33:559–78.
[23] Bishko G, McLeish TCB, Harlen OG, Larson RG. Phys Rev Lett 1997;79:2352–5.
[24] Vega DA, Milner ST. J Polym Sci, Part B: Polym Phys 2007;45:3117–36.
[25] Masubuchi Y, Matsumiya Y, Watanabe H, Shiromoto S, Tsutsubuchi M, Togawa Y. Rheol Acta 2012;51:193–200.
[26] Kempf M, Ahirwal D, Cziep M, Wilhelm M. Macromolecules 2013;46:4978–94.
[27] Snijkers F, Ratkanthwar K, Vlassopoulos D, Hadjichristidis N. Macromolecules 2013;46:5702–13.
[28] Vega DA, Gómez LR, Roth LE, Ressia JA, Villar MA, Valles EM. Phys Rev Lett 2005;95:166002.
[29] In reference 28, there is an error in Equation 1, and alpha should be replaced by 15/8.
[30] Langley NR. Macromolecules 1968;1:348–52.
[31] Langley N, Polmanteer K. J Polym Sci, Part B: Polym Phys 1974;12:1023–34.
[32] Pearson DS, Graessley WW. Macromolecules 1980;13:1001–9.
[33] Dossin LM, Graessley WW. Macromolecules 1979;12:123–30.
[34] Vallés EM, Macosko CW. Macromolecules 1979;12:673–9.
[35] Curro JG, Pearson DS, Helfand E. Macromolecules 1985;18:1157–62.
[36] Villar MA, Bibbo MA, Vallés EM. Macromolecules 1996;29:4072–80.
[37] Vega DA, Villar MA, Alessandrini JL, Valles EM. J Polym Sci, Part B: Polym Phys 1999;37:1121–30.
[38] Vega DA, Villar MA, Vallés EM, Steren CA, Monti GA. Macromolecules 2001;34:283–8.
[39] Acosta RH, Vega DA, Villar MA, Monti GA, Valles EM. Macromolecules 2006;39:4788–92.
[40] Urayama K, Kawamura T, Kohjiya S. Polymer 2009;50:347–56.
[41] Mrozek RA, Cole PJ, Otim KJ, Shull KR, Lenhart JL. Polymer 2011;52:3422–30.
[42] Yoo SH, Yee L, Cohen C. Polymer 2010;51:1608–13.
[43] Genesky GD, Cohen C. Polymer 2010;51:4152–9.
[44] Kan H-C, Ferry JD, Fetters LJ. Macromolecules 1980;13:1571–7.
[45] Granick S, Pedersen Nelb GW, Ferry JD. J Polym Sci, Part B: Polym Phys 1981;19:1745–57.
[46] Adachi K, Nakamoto T, Kotaka T. Macromolecules 1989;22:3111–6.
[47] Ndoni S, Vorup A, Kramer O. Macromolecules 1998;31:3353–60.
[48] Urayama K, Yokoyama K, Kohjiya S. Macromolecules 2001;34:4513–8.
[49] Bibbó MA, Vallés EM. Macromolecules 1984;17:360–5.
[50] Patel SK, Molone S, Cohen C, Gillmor JR, Colby RH. Macromolecules 1992;25:5241–51.
[51] Villar MA, Vallés EM. Macromolecules 1996;29:4081–9.
[52] Vega DA, Villar MA, Alessandrini JL, Valles EM. Macromolecules 2001;34:4591–6.
[53] Urayama K, Miki T, Takigawa T, Kohjiya S. Chem Mater 2004;16:173–8.
[54] Batra A, Cohen C, Archer L. Macromolecules 2005;38:7174–80.
[55] Acosta RH, Monti GA, Villar MA, Valles EM, Vega DA. Macromolecules 2009;42:4674–80.
[56] Yamazaki H, Takeda M, Kohno Y, Ando H, Urayama K, Takigawa T. Macromolecules 2011;44:8829–34.
[57] Yamaguchi M, Ono S, Okamoto K. Mater Sci Eng, B 2009;162:189–94.
[58] Vallés EM, Rost EJ, Macosko CW. Rubber Chem Technol 1984;57:55–62.
[59] Villar MA, Bibbó MA, Vallés EM. J Macromol Sci, Part A: Pure Appl Chem 1992;A29:391–400.
[60] Roth LE, Vega DA, Vallés EM, Villar MA. Polymer 2004;45:5923–31.
[61] Agudelo DC, Roth LE, Vega DA, Vallés EM, Villar MA. Polymer 2014;55:1061–9.
[62] Fetters LJ, Lohse DJ, Richter D, Witten TA, Zirkel A. Macromolecules 1994;27:4639–47.
[63] Steenbakkers RJA, Tzoumanekas C, Li Y, Liu WK, Kröger M, Schieber JD. New J Phys 2014;16:015027.
[64] Colby RH, Rubinstein M. Macromolecules 1990;23:2753–7.
[65] Ndoni S, Kramer O. Europhys Lett 1997;39:165–70.